

On the TDD Subframe Structure for Beyond 4G Radio Access Network

Eeva LÄHETKANGAS¹, Kari PAJUKOSKI¹, Esa TIIROLA¹, Gilberto BERARDINELLI²,
Ilkka HARJULA³, Jaakko VIHRIÄLÄ¹

¹ *Nokia Siemens Networks, Kaapelitie 4, 90620 Oulu, Finland*
Email: {eeva.lahetkangas,kari.pajukoski,esa.tirola}@nsn.com

² *Department of Electronic Systems, Aalborg University, Denmark*
Email: Gilberto.berardinelli.ext@nsn.com

³ *VTT Technical Research Centre of Finland, Kaitoväylä 1, 90570 Oulu, Finland*
Email: ilkka.harjula@vtt.fi

Abstract: The purpose of a Beyond 4G (B4G) radio access technology, is to cope with the expected exponential increase of mobile data traffic in local area (LA). The requirements related to physical layer control signaling latencies and to hybrid ARQ (HARQ) round trip time (RTT) are in the order of ~1ms. In this paper, we propose a flexible orthogonal frequency division multiplexing (OFDM) based time division duplex (TDD) physical subframe structure optimized for B4G LA environment. We show that the proposed optimizations allow very frequent link direction switching, thus reaching the tight B4G HARQ RTT requirement and significant control signaling latency reductions compared to existing LTE-Advanced and WiMAX technologies.

Keywords: Beyond 4G, TDD, OFDM, subframe, guard period, cyclic prefix

1. Introduction

While the standardization of 4th generation radio access technology (RAT) - namely Long Term Evolution – Advanced (LTE-A) [1] – is still ongoing, the discussion on a Beyond 4G (B4G) system has already started [1]. Within B4G timeframe, targeting year 2020, up to 1000 times increase in the total mobile data traffic, mostly generated by indoor subscribers, is foreseen in comparison to the current LTE-A Release 10. [2] The higher capacity requirements can be met by using a larger frequency spectrum with possibly higher carrier frequencies, by boosting the spectral efficiency and by increasing the number of cells; the latter option leads to a very dense small cell deployment and justifies the focus of B4G scope on local area (LA) networks. However, coping with the large B4G traffic demand is challenging from both cost and complexity point of view. In a previous contribution [2], we have listed the main system requirements for such B4G RAT. Latency reduction sets the B4G round trip time (RTT) requirement to the order of <1ms and can be seen as the main physical layer requirement to reach bit rates like 10Gbps with cost roughly on the same order as in today's systems. Also control signaling latency targets, including e.g. call setup, are strict; in LTE-A the required wake-up time (from idle to radio resource control (RRC)-connected state) is ~100ms when in B4G system it is in the range of ~10ms.

Due to the tight cost efficiency requirements of B4G, time division duplexing (TDD) is seen as a more attractive duplexing method with respect to frequency division duplex (FDD) due to larger amount of spectrum, the lower cost of the components and attractive properties such as reciprocity and good UL-DL scalability that can be utilized to create link-independent air interface and flexible resource partitioning. Framed access with

network synchronization, meaning that frames of different devices and cells in the network have concurrent timings, are needed for interference coordination as well as for achieving efficient resource usage and sharing. Thus, in the following, we focus on framed access on top of half-duplex TDD.

Orthogonal frequency division multiplexing (OFDM), enabling simple one-tap equalization at the receiver, straightforward extension to multiple input multiple output (MIMO) antenna techniques as well as low latency due to short time dispersion of the waveform, can be considered as the strongest candidate modulation for B4G [2]. OFDM suffers from overhead of cyclic prefix (CP) and guard band due to poor frequency localization and from high peak-to-average power ratio

In this paper, we examine how B4G LA environment and evolved component technology affect the B4G physical frame numerology by analysing significant parameters such as TDD guard period (GP) and CP. Based on this analysis as well as further design criteria, we propose a TDD subframe structure optimized for B4G LA networks and analyze its latency related benefits, such as reduced RTT of the enabled simplified HARQ scheme and UE initiated data transmission latency. Feasibility of existing LTE-A and WiMAX subframe structures and related signaling in B4G context are examined for reference.

The paper is organized as follows. In Section II we briefly present the physical frame structures and related latency limits of LTE-A and WiMAX. In Section III a proposal for a new B4G TDD subframe structure is presented. In section IV we give an overview of the main characteristics of B4G LA indoor environment together with evolved component technology, use this analysis to discuss the related B4G subframe dimensioning and analyze the simplified HARQ scheme and the latency limits enabled by the proposed subframe structure. Section V concludes the paper.

2. Frame Structure and Latency in LTE-A and WiMAX

In the following, frame structures and related latency restrictions of existing LTE-A and WiMAX technologies are presented. Our aim is to present significant reference cases for our B4G frame design.

2.1 – TDD LTE-A and WiMAX frame structures

In LTE-A, both FDD and TDD modes of operation are covered within the same set of 3GPP specifications. While these modes have been harmonized so that they both share the same underlying framework, transmission direction switching operation in TDD mode has led to few differences between their physical layers. The most significant TDD-specific feature is the frame structure, which introduces a special subframe. [3] TDD LTE-A frame, presented in Figure 1a, has been built on top of the LTE frame structure type 2. Subcarrier (SC) spacing of 15kHz is used, leading to OFDM symbol length of $66.7\mu\text{s}$. The frame structure has been optimized for wide area environment; the minimum CP duration is indeed set to $4.7\mu\text{s}$ and minimum switching time value per one switching point is $20.3\mu\text{s}$. One radio frame consists of 10 subframes, having 1ms duration each. The symbols dedicated to control information are always located at the beginning of the subframe, and their number can vary between 1 and 3. DL/UL direction switching is included in the form of the special subframe, which contains three fields: DL pilot time slot (DwPTS), GP and UL pilot time slot (UpPTS), whose lengths can be configured between 3-12, 1-10 and 1-2 OFDM symbols respectively. Two switching point periodicities, defining the hard limits for the two-way latency, namely 5ms and 10ms, are supported. The UL/DL switching ratio can be adjusted only with limited flexibility; 7 UL/DL configurations, presented in Table I, have been defined in 3GPP with DL:UL ratio varying from 2:3 to 9:1.

IEEE 802.16m (unofficially known as mobile WiMAX or WiMAX 2) also supports both FDD and (half-duplex) TDD operation modes. The new TDD frame structure specified in the IEEE 802.16m standard has been designed to shorten the transmission time intervals and to accelerate the HARQ retransmissions compared to the previous WiMAX system specified in the IEEE 802.16-2009 standard [4]. The main renewals, transparent to legacy devices, are the partitioning of the legacy radio frame into a number of subframes and the introduction of the concept of superframe and superframe header. The mobile WiMAX frame structure is presented in Figure 1b. A superframe has a 20ms duration and consists of a set of 4 consecutive and equally-sized radio frames. The standard allows utilizing different frame sizes, but typically the frame length is set to 5ms. The number of subframes per frame varies depending on the number of available OFDM symbols per frame, the CP size, and the transmission bandwidth. The number of switching points in each radio frame in TDD mode is limited to two, but different UL/DL ratios are supported. A frame with minimum supported CP configuration of $1/16 T_{symbol}$ contains 6 type-1 subframes, consisting of six OFDM symbols, and 2 type-2 subframes, consisting of seven OFDM symbols, for TDD for nominal channel bandwidths of 5, 10, and 20MHz. For these bandwidths, $T_{symbol} = 91.429\mu s$. The Transmit (TX)/Receive (RX) Transition Gap (TTG) and RX/TX Transition Gap (RTG) take $142.853\mu s$ altogether, while minimum transition gap time per one switching point is restricted to $5\mu s$.

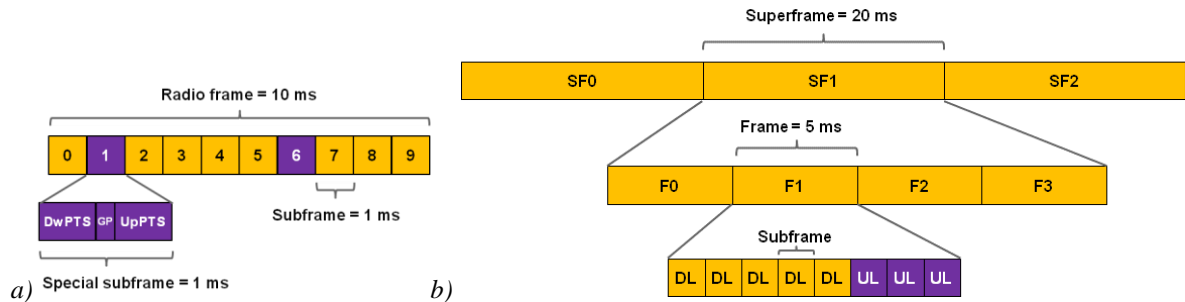


Figure 1. Frame structure of TDD a) LTE-A, b) WiMAX.

2.2 – HARQ structure and latency

HARQ technique enables faster recovery from errors in cellular networks by combining traditional automatic repeat request (ARQ) error control, where redundant bits are added to the transmitted data using an error-detecting code, with forward error correction (FEC) coding. The parity bits are either sent immediately along with the original message or transmitted upon request when an erroneous message is detected by the receiver. In addition, soft combining can be utilized, meaning that incorrectly received coded data blocks are stored by the receiver and combined with the retransmitted blocks for decoding. Both LTE-A and WiMAX use synchronous HARQ in UL and asynchronous HARQ in DL direction.

In LTE-A FDD mode the HARQ RTT time, (i.e., the time between the data grant and the time instant when next grant/packet can be sent after the corresponding HARQ acknowledgement, ACK) is constant (8ms). In TDD mode, corresponding HARQ RTT with comparable number of HARQ retransmissions is clearly worse and varying according to link direction, UL/DL configuration and subframe number. The number of LTE-A TDD HARQ processes varies between 4 and 15 for DL and between 1 and 7 for UL [5]. The eNB or UE, upon detection of data transmission in subframe n , will transmit the corresponding ACK in subframe $n+k$, where k is given in TABLE I, allowing 3ms processing time at eNB and UE for both data and HARQ (N)ACK processing and leading the total HARQ RTT to be variant on up to 16ms. In many cases several ACKs may need to be transmitted within

one subframe, leading to increasing complexity related to variable HARQ ACK payloads, HARQ ACK resource allocation and timing and error case handling.

Table 1: LTE-A TDD DL/UL HARQ timings.

UL/DL configuration	Switching periodicity	DL&UL ACK/NACK timing index k									
		Subframe n				DL: k for UL ACK			UL: k for DL ACK		
		0	1	2	3	4	5	6	7	8	9
0	5ms	4	6	4	7	6	4	6	4	7	6
1		7	6	4	6	4	7	6	4	6	4
2		7	6	6	4	8	7	6	6	4	8
3	10ms	4	11	6	6	6	7	6	6	5	5
4		12	11	6	6	8	7	7	6	5	4
5		12	11	6	9	8	7	6	5	4	13
6	5ms	7	7	4	6	6	7	7	4	7	5

In WiMAX, the maximum number of HARQ channels is 16 for both UL and DL. The exact method for calculation of HARQ timings is given for example in [4], and not repeated here. Basically, the limiting factor for HARQ RTT time, illustrated in Figure 2, is the frame length. By assuming 3 subframes of processing time, the DL HARQ ACK can be received from the UE within the same frame where the HARQ packet is transmitted, yielding the HARQ RTT of 5ms. In UL HARQ, the UE must have the assignment from the BS before the HARQ packet transmission, but the RTT for the actual HARQ process is similarly 5ms. In practice the RTT is higher in most of the cases, as there are usually several HARQ channels running, and the placement of the HARQ packets that minimizes the RTT might not be possible for all the channels simultaneously.

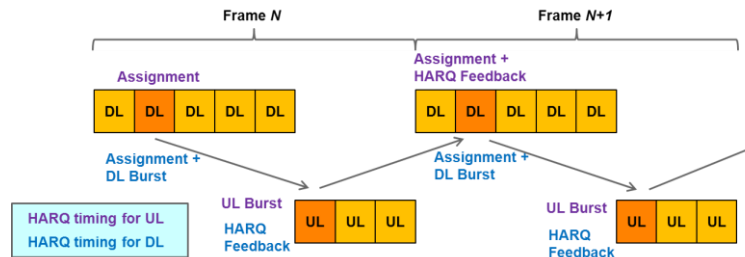


Figure 2. HARQ timing for WiMAX DL and UL.

2.3 – UE initiated data transmission latency

When considering UE initiated data transmission of LTE-A, UE is assumed to be in RRC connected state and have radio bearers established. Figure 3 presents the needed signaling. If UE is already synchronized to eNB, it needs to first wait for the PUCCH allocation for sending the scheduling request (SR). SR is received and processed by eNB, which then generates an UL scheduling grant (SG) and sends it to UE. The SG is decoded by UE and used for sending the actual UL data to eNB. Time spent for UE initiated data transmission in TDD LTE-A depends on the used UL/DL configuration. For example when UL/DL configurations with 5ms periodicity are used, at least 13.5ms is needed in case of synchronized UE, assuming processing times of 3ms in both eNB and UE for SR and SG handling. [6] Even if the SR and SG processing times would theoretically be decreased to 1 subframe, the limitations in UL/DL switching periodicity in LTE-A frame structure would restrict the UE initiated data transmission duration to 7.5ms at minimum.

When considering UE initiated data transmission in WiMAX, UE is assumed to be in connected state and in active mode. In IEEE 802.16m, the random access bandwidth request (BR) process can be carried out in minimum of three steps, resembling closely the corresponding process in LTE-A, illustrated in Figure 3, with BR preamble corresponding to SR and BR-ACK A-MAP IE corresponding to SG of LTE-A. We can calculate that at

least one full frame of 5ms is consumed, assuming that the UE can utilize the BR channel in the beginning of the UL part of the frame, BS decodes the BR during the UL transmission, transmits the BR-ACK A-MAP IE in the next DL frame, and allocates the UE the requested bandwidth at the beginning of next UL frame. In practice, the UE has to wait for the BR opportunity, so the time required for the UE initiated data transmission is longer.

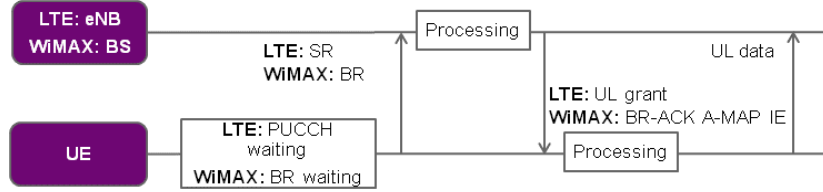


Figure 3. Signaling of UE initiated data transmission.

3. B4G Physical Subframe Proposal

The tight latency requirements of B4G system lead to short RTT with fast control signaling, fast TDD switching periodicity and support for flexible UL/DL ratio. A proposal for a TDD optimized physical subframe structure for B4G system is given in Figure 4. Only one TDD type is presented here, in the other TDD mode the transmission (TX) and receiving (RX) phases are in the opposite order. In order to enable robust and fast control plane, control signaling is embedded to each subframe and time separated from the data plane. Control symbols are located before data symbols in order to allow fast and cost efficient pipeline processing at the receiver. It is possible to use different SC spacing, coding and modulation schemes for control and data planes. Control part of the subframe provides possibility to include both RX and TX resources for control, allowing the devices in the network to both receive and send control signals, such as SRs and SGs, in every subframe. TX and RX control parts are proposed to be symmetrical in order to enable link independent multiple access. In addition to scheduling related control information, control plane may also contain reference signals (RS), used for cell detection and selection, frequency domain scheduling, precoder selection and channel estimation. Rest of the subframe after the control part is dedicated for data plane. In order to achieve low complexity, data part in one subframe contains only transmitting or receiving possibility for data symbols.

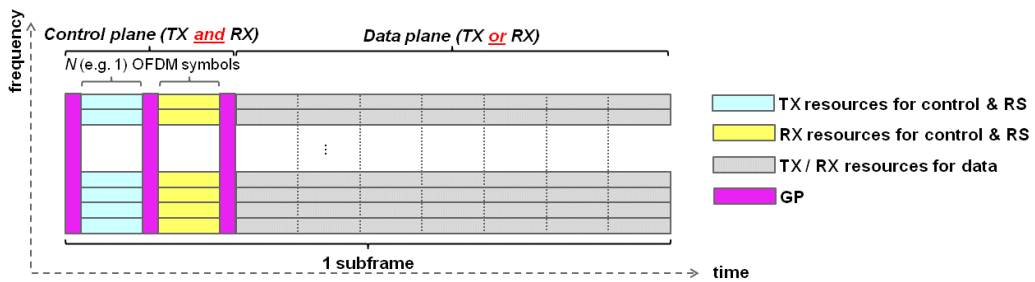


Figure 4. Proposed B4G physical subframe structure.

In order to allow fully flexible allocation of different control and data part patterns for consecutive subframes, TX and RX control parts need to be separated from each other and from the data symbols with a GP, leading to total number of 3 GPs per subframe. Assuming symmetrical TX and RX control parts with N_{ctrl_s} symbols in each and defining that same SC spacing is used for control and data planes, with N_{data_s} being the number of data symbols and T_{symbol} being the length of an OFDM symbol, the subframe length T_{sf} can be determined as

$$T_{sf} = (2 \cdot N_{ctrl_s} + N_{data_s}) \cdot (T_{symbol} + T_{CP}) + 3 \cdot T_{GP} . \quad (1)$$

4. Dimensioning and Latency of B4G Subframe

In the following, we shortly analyze how optimization to B4G LA environment and evolved component technology affect the B4G physical frame numerology. In addition, while still leaving the design of control and RS structure for further study, we provide a brief numerical example-based analysis to show the feasibility of the proposed subframe structure even with short subframe lengths. Based on this analysis we then examine the related HARQ and UE initiated data transmission latencies.

4.1 – B4G LA radio channel and evolvments in component technology

As mentioned in the introduction, a dense deployment of small indoor cells working in dedicated spectrum is foreseen for a B4G RAT. Cell radius, multipath propagation and penetration losses through walls and floors are the main causes for signal attenuation and fading in the radio channel, together with increased pathloss due to possible usage of higher carrier frequencies [7]. The size of a typical LA cell radius is anticipated to be around ~50m, corresponding to propagation delay, $T_{CH_{pr}}$, of ~170ns. Short propagation delay implies that precise timing control procedures ensuring the concurrent reception timings of UEs in the different parts of the cell, such as timing advance (TA), may not be needed in case the CP is long enough for coping with them. Also, compared to outdoor and macro cells, channel delay spread, $T_{CH_{ds}}$, interpreted as the arrival time difference between the earliest and the last significant multipath component, of LA indoor channels is much shorter. The typical r.m.s. channel delay spread (the standard deviation value of the delay of reflections, weighted proportional to the energy in the reflected waves) is typically <100ns for office premises. The filter response to delay spread in transmitter and receiver, T_{HW_f} , in radio channels with small delay spread is estimated to be ~50ns.

In a TDD device, the receiver may be interfered by the transmitter due to ramp-on and ramp-off delays of the power amplifier. TDD hardware (HW) switching time, T_{HW_s} , contains both the rise/fall times, needed by the device to switch to/from 90% from/to 10% nominal power, and the so called gate lag time, needed to switch from the last 10% nominal power to adequate near-zero level. In [8], a wireless LA network switch with rise/fall times of 13ns and gate lag of 27ns is presented and in [9] it has been shown that gate lag times less than 20ns can be achieved. Consequently, it is reasonable to expect that TDD switches supporting $T_{HW_s} < 60$ ns will be broadly available in products in B4G timeframe. Also, the digital signal processing performance is expected to increase according to Moore's law [10], enabling more than 10 times increase in the execution speed of fast Fourier transform compared to the current component benchmarking values. This enables relatively low SC spacing even with large B4G bandwidths.

4.2 – B4G TDD Numerology: GP and CP

Existing standards such LTE-A and WiMAX, whose frame numerologies have been previously presented, are not designed for LA environment and have legacy burden restrictions when utilizing evolving component technology. The B4G environment properties together with evolved component technology aspects enable instead the usage of shorter and B4G optimized GP and CP times. [7]

GP is allocated to the transmission direction switching point in order to obtain a sufficient off power of the transmitter (avoid power leakage in the receiver chain) and in order to compensate cell size-dependent propagation delay $T_{CH_{pr}}$ and delay spread $T_{CH_{ds}}$, together with corresponding delay spread filter response time T_{HW_f} in transmitter and receiver. The time required for GP in B4G TDD system can be then estimated as

$$T_{GP} \approx T_{CH_{ds}} + T_{CH_{pr}} + T_{HW_s} + T_{HW_f} = 100\text{ns} + 170\text{ns} + 60\text{ns} + 50\text{ns} = 380\text{ns} < 0.5\mu\text{s}. \quad (2)$$

In OFDM systems, inter-symbol and inter-carrier interference due to time-dispersive channel propagation is prevented by allocating a CP to each OFDM symbol. The CP duration is determined so that it exceeds the delay spread in the environment where the system is intended to operate and compensates the impact of transmitter and receiver filters. In addition, CP design is also intended to cope with synchronization mismatches and timing errors in the cell. Since precise timing control procedures, such as TA, are not used due to the limited propagation delay in LA and since UE is synchronized to DL signal, the time uncertainty that needs to be compensated within the CP can be estimated as a two-way maximum propagation delay. T_{sync_err} parameter presents synchronization error and has been estimated as $\sim 500\text{ns}$ to ensure a safe margin to compensate for misalignment errors between cells. The required total B4G CP time, TCP_B4G, can therefore be estimated as

$$\begin{aligned} T_{CP} &\approx T_{CH_{ds}} + 2 \cdot T_{CH_{prop}} + T_{HW_f} + T_{sync_err} \\ &= 100\text{ns} + 2 \cdot 170\text{ns} + 50\text{ns} + 500\text{ns} = 990\text{ns} < 1.0\mu\text{s}. \end{aligned} \quad (3)$$

4.3 – Control overhead and subframe length analysis

The size of the control part of the proposed physical subframe is heavily dependent on the environment and used deployment. There should be enough RS resources to guarantee feasible amount of orthogonal RS sequences and sufficient RS power even in the cell edge. There should also be enough resources for scheduling and HARQ signaling, depending on the amount of UEs in the cell. In the following we propose an example subframe numerology where 1 OFDMA symbol is reserved for both TX and RX control in a subframe with 14 symbols in total, assuming 60kHz SC spacing. One control symbol can be assumed to be sufficient in B4G environment due to decreased number of UEs in dense deployment cells and due to more available spectrum and the expected large coherence bandwidth, which allows a larger RS spacing in frequency. With the proposed approach, where $N_{ctrl_s}=1$ with 60kHz SC spacing, we can easily define an example subframe with length of 0.25ms, leading to GP value of $0.89\mu\text{s} > 0.5\mu\text{s}$ (fulfilling the minimum GP requirement). The total percentage of overhead per 0.25ms subframe can be calculated as

$$\begin{aligned} \text{Overhead} &= (2 \cdot N_{ctrl_s} \cdot T_{symbol} + (2 \cdot N_{ctrl_s} + N_{data_s}) \cdot T_{CP} + 3 \cdot T_{GP}) / T_{sf} \cdot 100 \\ &= (2 \cdot 1 \cdot (1/60\text{kHz}) + (2 \cdot 1 + 12) \cdot 1\mu\text{s} + 3 \cdot 0.89\mu\text{s}) / 250\mu\text{s} \cdot 100 = 20\%, \end{aligned} \quad (4)$$

which can be considered still as a feasible overhead value. Thus, it can be estimated that the proposed physical subframe structure allows usage of low subframe lengths, such as 0.25ms, with reasonable overhead and with sufficient resources for control and RS. Figure 5 illustrates the overhead of the proposed B4G subframe as a function of subframe length when keeping the amount of control symbols fixed. Curves with the minimum CP and GP numerology of LTE-A and WiMAX have also been plotted for reference, illustrating that the suggested B4G subframe structure with short subframe length would not be feasible with the CP and GP numerology of the existing standards.

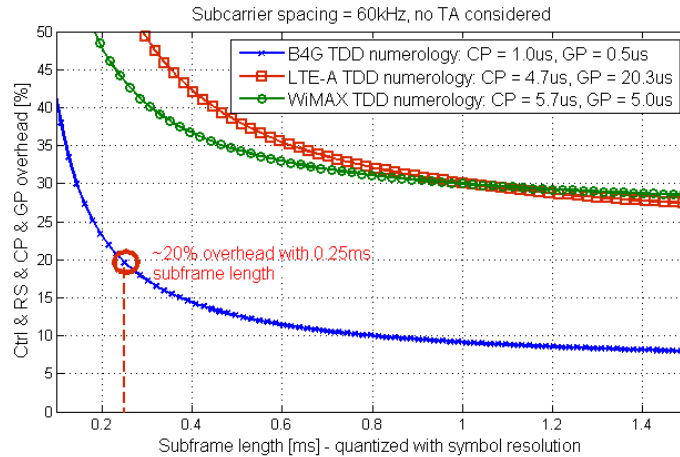


Figure 5. Overhead of the proposed B4G subframe structure as a function of subframe length.

4.4 – HARQ and UE initiated data transmission latency

The simplified control plane and its presence in each subframe enables a clean TDD HARQ scheme with HARQ timing not dependent on the UL/DL ratio. HARQ timing can be fixed and counted in subframe(s), which remarkably reduces TDD HARQ complexity compared to existing technologies and decreases the related HARQ latency. The HARQ schemes for both traditional DL and UL directions, with scheduling for both links done by eNB, are illustrated in Figure 6 using the proposed subframe structure from eNB's point of view. It is visible that for HARQ RTT, 4 subframes are needed in both DL and UL. Using the earlier conclusion that $\sim 0.25\text{ms}$ subframe length is feasible, the total HARQ RTT enabled by the proposed subframe structure is therefore $\leq 1\text{ms}$. The reduced HARQ latency further enables usage of fewer HARQ processes compared to LTE-A and WiMAX, reducing also memory consumption and device cost since less receiver HARQ buffers are needed and HARQ buffering forms a remarkable part of the baseband cost.

Since physical subframe contains both TX and RX opportunities for control information, each subframe may contain separate HARQ processes for different link directions. Existence of the link direction specific HARQ processes can be determined on-necessity basis, depending for example on the used UL/DL ratio, and the processes can be designed to be asynchronous. Due to its link independent nature, the enabled HARQ arrangement is also well-suited for multi-hop scenarios by allowing the chaining of the HARQ entities in such a way that each hop (both link directions included) has its own HARQ loop with dedicated configurations, such as different number of HARQ processes and timing offsets between data allocation and HARQ acknowledgement.

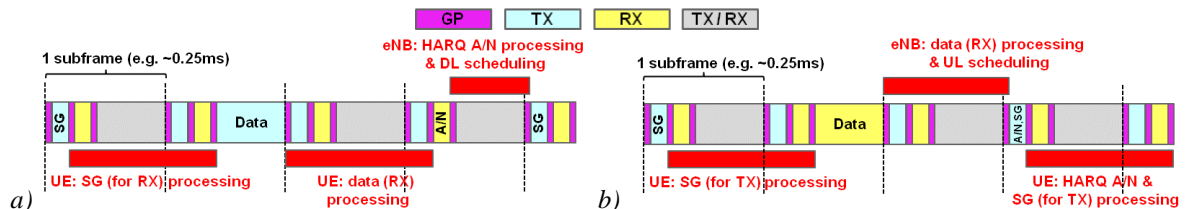


Figure 6. HARQ scheme with proposed subframe structure with data transmission to a) DL, b) UL direction.

The proposed subframe structure allows also to decrease the latency of other control signaling and handshakes, such as related to UE initiated data transmission. Like illustrated in Figure 7, this handshake requires at least 3.5 TDD subframes, assuming that processing times are less than data part duration in one subframe; on average ~ 0.5 subframes for SR opportunity waiting, one subframe for SR, one for SG and one for actual data. Assuming

that $\sim 0.25\text{ms}$ subframe length is in use, the total theoretical minimum UE initiated data transmission latency is $< 1\text{ms}$.

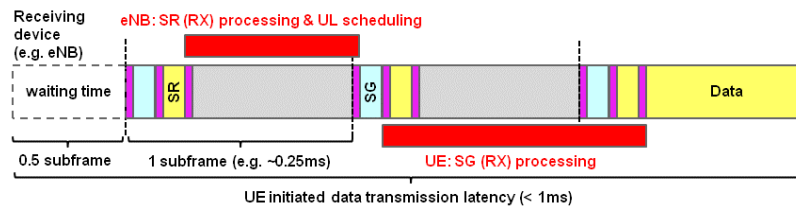


Figure 7. UE initiated data transmission with proposed B4G physical subframe structure.

The improvements provided by the proposed B4G subframe structure in terms of link direction switching periodicity together with decreased HARQ RTT and control signaling latency have been summarized in Figure 8. Corresponding minimum latency values of LTE-A have been plotted for reference (WiMAX values are comparable to LTE-A). While the practical total latency is very dependent on the processing capabilities of the devices, the proposed B4G subframe structure provides flexibility in terms of supported processing times and enables remarkably lower latencies compared to corresponding LTE-A and WiMAX schemes.

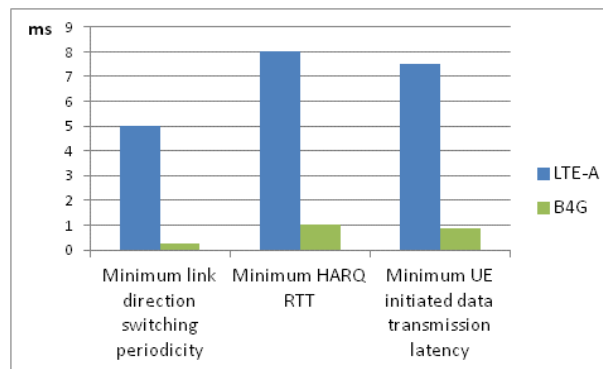


Figure 8. Minimum latencies enabled by the proposed B4G subframe structure (in comparison to LTE-A).

5. Conclusions

In this paper, we proposed a physical TDD subframe structure for B4G system, optimized for B4G LA environment bearing in mind the expected evolvments in the component technology. For the time being, we focused on the time dimension of the subframe structure, leaving frequency positioning and allocation for further study. The proposed subframe structure with time-separated control plane is feasible even with low subframe lengths and allows more frequent link direction switching. This further enables achieving the tight B4G HARQ RTT requirement of 1ms and significant control signaling latency reductions not feasible with existing LTE-A and WiMAX technologies.

Acknowledgements

This work has been performed in the framework of the FP7 project ICT-317669 METIS.

References

- [1] H. Holma and A. Toskala, LTE for UMTS – Evolution to LTE-Advanced, 2nd ed., Wiley, 2011.
- [2] P. Mogensen, K. Pajukoski, B. Raaf, E. Tiirola, E. Lähetkangas, I.Z. Kovács, G. Berardinelli, L.G.U. Garcia, L. Hu, A.F. Cattoni, “B4G local area: high level requirements and system design”, IEEE Globecom, 2012.
- [3] “TD-LTE: Exciting Alternative, Global Momentum,” White paper, Motorola, 2010.
- [4] S. Ahmadi, Mobile WiMAX – A Systems Approach to Understanding IEEE 802.16m Radio Access Technology, Elsevier, 738 p., 2011.

- [5] 3GPP TS 36.213 v.10.8.0, Physical layer procedures for Evolved Universal Terrestrial Radio Access (E-UTRA). Available: www.3gpp.org.
- [6] D. Singhal, M. Kunapareddy, V. Chetlapalli, "LTE-Advanced: Latency Analysis for IMT-A Evaluation", White paper, Tech Mahindra Limited, 2010.
- [7] E. Lähetkangas, K. Pajukoski, G. Berardinelli, F. Tavares, E. Tiirola, I. Harjula, P. Mogensen, B. Raaf, "On the Selection of Guard Period and Cyclic Prefix for Beyond 4G TDD Radio Access Network", submitted to European Wireless, 2013.
- [8] M/A-COM Technology Solutions, MASW-009590-000DIE data sheet. Available: <http://www.macomtech.com/datasheets/MASW-009590.pdf>.
- [9] A. Freeston, C. Varmazis, T. Boles, "Nanosecond pHEMT switches," European Microwave Integrated Circuits Conference, 2009.
- [10] S. Borkar and A. Chien, "The Future of Microprocessors," Communications of ACM, vol. 54, no.5, 2011.